

The transition from the classical to the quantum regime in nonlinear Landau damping.

¹G. Brodin, ¹J. Zamanian, ²J. T. Mendonca

¹*Department of Physics, Umeå University, SE-901 87 Umeå, Sweden,*

²*IPFN, Instituto Superior Tecnico, 1049-001 Lisboa, Portugal*

Starting from the Wigner-Moyal equation coupled to Poisson's equation, a simplified set of equations describing nonlinear Landau damping of Langmuir waves is derived. This system is studied numerically, with a particular focus on the transition from the classical to the quantum regime. In the quantum regime several new features are found. This includes a quantum modified bounce frequency, and the discovery that bounce-like amplitude oscillations can take place even in the absence of trapped particles. The implications of our results are discussed.

I. INTRODUCTION

Numerous aspects of quantum plasmas have been investigated during the last decade, see e.g. [1–3]. Basic features such as electron degeneracy and particle dispersive properties have been studied in some detail [1–9]. Exchange effects [10, 11], the magnetic dipole force and other contributions from the electron spin [12, 13] have also been examined, including relativistic effects [14, 15]. Systems of interest in this context include e.g. quantum wells [16], laser-plasma interaction on solid density targets [17], and astrophysical plasmas [18]. Works on quantum plasmas also have relevance for recent applications in plasmonics [19] and spintronics [20].

In the present paper we will consider the influence of quantum effects on the nonlinear regime of Landau damping, based on the Wigner-Moyal equation [2] that accounts for particle dispersive effects. Previous works in this area [21, 22] have deduced that quantum effects can suppress the nonlinear bounce oscillations of Langmuir waves and turn the evolution into basic linear damping. Moreover, quantum corrections to electron holes in phase space that may form as a result of wave-particle interaction have been calculated in Ref. [23], and the quasilinear theory of the Wigner-Poisson system has been studied in Ref. [24]. However, many of the details of nonlinear Landau damping have not been studied before in the quantum regime. Making analytical approximations applicable for a resonance in the tail of the distribution, we first simplify the Wigner-Moyal equation coupled to Poisson's equation into a system that is more easy to solve numerically. This system is shown to fulfill an energy conservation law, and reduces to a previously studied system [25] in the classical limit. A systematic study of the transition from classical to quantum behavior then reveals several new features. This include a quantum modification of the bounce frequency, a new condition for the quantum suppression of the nonlinear regime and the discovery that bounce-like oscillations can take place even in the absence of trapped particles.

Similar to most cases, the conditions needed for quantum effects to be important in our problem include a high plasma density and a modest plasma temperature. However, while the scaling with temperature and density is the same as usual [1, 3], the precise numerical values are to some extent relaxed compared to the standard expressions in case the resonance lies in the tail of the distribution. The general conclusion is that the properties of wave-particle interaction are more easily influenced by quantum effects than the ordinary fluid properties. A concrete example is provided in the final section, and the significance of our results are discussed.

II. BASIC EQUATIONS AND DERIVATIONS

Our starting point is the Wigner-Moyal equation [2], which reads

$$\frac{\partial f}{\partial t} + \mathbf{v} \cdot \nabla f - \frac{iq}{\hbar} \int \frac{d^3 \mathbf{r}' d^3 \mathbf{v}' m^3}{(2\pi\hbar)^3} e^{i\mathbf{r}' \cdot (\mathbf{v} - \mathbf{v}') m/\hbar} [\Phi(\mathbf{r} + \mathbf{r}'/2) - \Phi(\mathbf{r} - \mathbf{r}'/2)] f(\mathbf{r}, \mathbf{v}', t) = 0 \quad (1)$$

Here f is the Wigner-function, Φ is the electrostatic potential, q ($=-e$) is the electron charge, m is the electron mass and $\hbar = 2\pi\hbar$ is Planck's constant. Eq. (1) is combined with Poisson's equation

$$-\nabla^2 \Phi = \frac{q}{\varepsilon_0} \int f d^3 \mathbf{v} \quad (2)$$

to give us a closed set. Eq. (1) applies for electrostatic fields and do not account for the spin of the electrons or exchange effects. For generalizations to electromagnetic fields and spin effects, see e.g. Ref. [12] and for generalizations to include exchange effects, see e.g. [11]. Here we focus on the problem of Langmuir waves in an unmagnetized plasma, in which case the omissions of electromagnetic effects and spin effects are trivially justified. Furthermore, we will consider the case of a moderate plasma density with $\hbar\omega_p \ll k_B T$. It is then safe to exclude exchange effects [11]. In fact, the condition $\hbar\omega_p \ll k_B T$ is often used also to disregard the particle dispersive quantum effects included in Eq. (1). Such a condition is indeed an appropriate one for neglecting e.g. the particle dispersive contribution to the real part of the Langmuir dispersion relation and for neglecting the quantum contribution of Eq. (1) in many other cases [1–3]. However, as we will see below, the quantum contribution to wave particle interaction can be crucial even in the regime $\hbar\omega_p \ll k_B T$. A useful starting point to see this is to rewrite (1) in the alternative way [26]

$$\frac{\partial f}{\partial t} + \mathbf{v} \cdot \nabla - \frac{q}{m} \Phi \cdot \left[\frac{2m}{\hbar} \sin \left(\frac{\hbar}{2m} \frac{\overleftarrow{\partial}}{\partial \mathbf{r}} \cdot \frac{\overrightarrow{\partial}}{\partial \mathbf{v}} \right) f \right] = 0. \quad (3)$$

Here the arrows on the operators indicate in which direction they are acting, and the sinus-operator is defined in terms of its Taylor-expansion. Let us first consider linear plane wave solutions $\propto \exp i(kz - \omega t)$, and estimate the

relative importance of quantum corrections. Letting $f = f_0 + \hat{f}_1 \exp i(kz - \omega t)$ we can use the classical linear solution

$$\hat{f}_1 = \frac{qk\hat{\Phi}}{m(\omega - k_z v_z)} \frac{\partial f_0}{\partial v_z} \quad (4)$$

as a means to illustrative the importance of quantum corrections. Comparing the magnitude of the first order quantum correction in the Taylor expansion with that of the classical term, we note that in the bulk of the velocity distribution (i.e. for $v \sim v_t$) the quantum corrections are small provided $Q_{\text{bulk}} \ll 1$, where

$$Q_{\text{bulk}} = \frac{\hbar k}{mv_t}. \quad (5)$$

However, looking at velocities close to the wave-particle resonance we must let $\omega - k_z v_z$ be small, of the order $\omega - k_z v_z \sim \gamma_L$ where γ_L is the linear damping rate. Close to the resonance the relative importance of the quantum terms are given by the parameter Q_{res} , which is

$$Q_{\text{res}} = \frac{\hbar k^2}{m\gamma_L}. \quad (6)$$

For a resonance in the tail of the distribution $\gamma_L/k \ll v_t$ in which case we may have $Q_{\text{res}} \sim 1$ at the same time as $Q_{\text{bulk}} \ll 1$. This regime will be the focus in what follows. As a result it suffices to solve the Vlasov limit of Eq. (3) in most of velocity space, but close to the resonance we need to solve the full Wigner equation. A similar approach applies for the small amplitude approximations. Provided $qk\hat{\Phi}/m\omega v_t \ll 1$ we have $|\partial \hat{f}_1 / \partial v_z| \ll |\partial f_0 / \partial v_z|$ unless we are close to the resonance. We will assume $qk\hat{\Phi}/m\omega v_t \ll 1$ to hold, and thus for most of velocity space we can solve the *linearized Vlasov relation*. However, close to the resonance where we can have nonlinear wave-particle interaction we must solve the *Wigner equation without making linear approximations*.

For a resonance in the tail of the distribution the number of particles contributing to the nonlinear interaction are relatively few. As a result there will be only minor harmonic generation of the electric field. Consequently we will use the ansatz of a slowly time-varying plane wave $\Phi = \hat{\Phi}(t) \exp i(kz - \omega t) + \text{c.c.}$ for the potential, where c.c. stands for complex conjugate. In general the Wigner function will be a periodic function, that will be represented as

$$f = f_0(\mathbf{v}) + \delta f_0(\mathbf{v}, t) + \left[\sum_{n=1}^{\infty} f_n(\mathbf{v}, t) \exp i[n(kz - \omega t)] + \text{c.c.} \right].$$

Next we divide the velocity space into the resonant region $[v_z - \delta v_{\text{res}}, v_z + \delta v_{\text{res}}]$ and the non-resonant region containing the complementary part. When evaluating the charge density in (2) we thus use $\int f d^3v = \int_{\text{nr}} f d^3v + \int_{\text{res}} f d^3v$ where the subscripts nr and res denotes the nonresonant and resonant regions, respectively. Since the linear Vlasov equation applies in the nonresonant region we can use

$$\begin{aligned} \int_{\text{nr}} f d^3v &= \int_{\text{nr}} f_1(\mathbf{v}, t) e^{i(kz - \omega t)} d^3v + \text{c.c.} = \\ &= \frac{qk\hat{\Phi}(t)}{m} \int_{\text{nr}} \frac{e^{i(kz - \omega t)} (\partial f_0 / \partial v_z)}{(\omega - k_z v_z)} d^3v - \int_{\text{nr}} \frac{e^{i(kz - \omega t)} (\partial f_1 / \partial t)}{i(\omega - k_z v_z)} d^3v + \text{c.c.} \end{aligned} \quad (7)$$

Noting that the second term on the right hand side of (7) is a small correction, proportional to the slowly varying amplitude, we can use the lowest order approximation (i.e. dropping time derivatives on the amplitude) to convert it to a term proportional to $\partial \hat{\Phi}(t) / \partial t$. Combining (7) with (2) we then deduce

$$\frac{\partial \hat{\Phi}(t)}{\partial t} = \frac{q}{\varepsilon_0 k^2 \partial D / \partial \omega} \int_{\text{res}} f_1 d^3v \quad (8)$$

where $D(\omega, k) = 1 + (q^2 / km\varepsilon_0) \int_{\text{nr}} (\partial f_0 / \partial v_z) d^3v / (\omega - k_z v_z)$. Note that the dispersion function $D(\omega, k)$ has a component of arbitrariness in the definition, since it depend on the width of the resonant region δv_{res} . Nevertheless in the derivation of (8) we have taken $D(\omega, k) = 0$ to hold by definition (i.e. $\omega(k)$ is defined by this relation), and in case a possible frequency shift occurs due to this, it is included in the time-dependence of $\hat{\Phi}$. It should be stressed that although a large number, of harmonics $f_n(\mathbf{v}, t)$ might be needed to solve for the Wigner function in the resonant region, it is only the first harmonic f_1 that contributes in (8).

Next we need to solve for the Wigner function in the resonant region. We restrict ourselves to a Maxwellian background distribution $F_0(\mathbf{v})$, and introduce the 1D-Wigner function

$$g = G_0(v_z) + g_0(v_z, t) + \left[\sum_{n=1}^{\infty} g_n(v_z, t) \exp i[n(kz - \omega t)] + \text{c.c} \right] \quad (9)$$

where $F_0(\mathbf{v}) = G_0(v_z) \exp[(-v_x^2 - v_y^2)/v_t^2]$ and $f_n(\mathbf{v}, t) = g_n(v_z, t) \exp[(-v_x^2 - v_y^2)/v_t^2]$. This ansatz is then substituted into (3). Since the gradient operator becomes $\pm ik\hat{\mathbf{z}}$ (as the spatial dependence of the potential is $\exp(\pm ikz)$) a useful formula is

$$\frac{2m}{\hbar} \sin \left(\pm \frac{i\hbar k}{2m} \frac{\partial}{\partial v_z} \right) g_n(v_z, t) = \frac{\pm im [g_n(v_z + \hbar k/2m) - g_n(v_z - \hbar k/2m)]}{\hbar}. \quad (10)$$

With the help of this formula, and substituting the ansatz (9) into (3), the following set of coupled equations are deduced

$$\begin{aligned} \frac{\partial g_1}{\partial t} - i\delta\omega(v_z)g_1 &= \frac{q}{\hbar} \hat{\Phi} [G_0(v_z + \hbar k/2m) - G_0(v_z - \hbar k/2m) + g_0(v_z + \hbar k/2m) - g_0(v_z - \hbar k/2m)] \\ &\quad + \hat{\Phi}^* [g_2(v_z + \hbar k/2m) - g_2(v_z - \hbar k/2m)] \end{aligned} \quad (11)$$

$$\frac{\partial g_n}{\partial t} - in\delta\omega(v_z)g_n = \frac{q}{\hbar} \hat{\Phi} [g_{n-1}^*(v_z + \hbar k/2m) - g_{n-1}^*(v_z - \hbar k/2m)] + \hat{\Phi}^* [g_{n+1}(v_z + \hbar k/2m) - g_{n+1}(v_z - \hbar k/2m)] \quad (12)$$

and

$$\frac{\partial g_0}{\partial t} = \frac{q}{\hbar} \hat{\Phi} [g_1^*(v_z + \hbar k/2m) - g_1^*(v_z - \hbar k/2m)] + \hat{\Phi}^* [g_1(v_z + \hbar k/2m) - g_1(v_z - \hbar k/2m)] \quad (13)$$

where $\delta\omega(v_z) = \omega - kv_z$ and the star denotes complex conjugate. Using $\int_{\text{res}} f_1 d^3v = \pi v_t^2 \int_{\text{res}} g_1 dv_z$ in (8) we see that Eqs. (11)-(13) and (8) constitute a closed set. The equations agree with those studied by Ref. [25] in the classical limit $\hbar \rightarrow 0$, provided the collisional frequency is put to zero in that work. It is clear that the quantum features are encoded in the velocity shift $\hbar k/2m$. An important thing to note is that we can use $G_0(v_z + \hbar k/2m) - G_0(v_z - \hbar k/2m) \approx [\partial G_0(v_z)/\partial v_z] \hbar k/m$ for $\hbar\omega/mv_t^2 \ll 1$, whereas similar approximations are not applicable for the perturbed Wigner function, as the quantities g_n varies on a much shorter scale length.

Before we can proceed we must put constraints on the parameter δv_{res} . For the resonant region to cover a sufficient amount of resonant particles in the linear regime we need the condition $\delta v_{\text{res}} \gg \gamma_L/k$. Moreover, to cover particles that are closed to be trapped in the potential well with a sufficiently large margin we need $\delta v_{\text{res}} \gg \omega_B/k$, where $\omega_B = (qk^2\Phi/m)^{1/2}$ is the bounce frequency of trapped particles (with this choice the resonant region is at least an order of magnitude larger than the region of trapped particles). Finally, to cover the quantum effects properly we need $\delta v_{\text{res}} \gg \hbar k/2m$. At the same time the calculation scheme is based on the resonance region being much smaller than the thermal velocity, and hence we need $\delta v_{\text{res}} \ll v_t$. If we sharpen this condition slightly and limit ourselves to $\delta v_{\text{res}} \ll kv_t^2/\omega$ we may take $[\partial G_0(v_z)/\partial v_z]$ as constant in the resonance region ($= [\partial G_0(v_z)/\partial v_z]_{\omega/k}$), which simplify some of the technical aspects. For a resonance that lies in the tail of the distribution we can have $kv_t/\gamma_L \gtrsim 100$, in which case it is easy to fulfill all conditions simultaneously, unless the nonlinearity or the quantum effects are extremely strong. Importantly, the numerical solutions presented below are not dependent on the precise choice of δv_{res} , as long as the above conditions are fulfilled.

Next we introduce normalized variables. Choosing normalized time as $\gamma_L t$, normalized velocity as kv_z/γ_L , normalized potential as $qk^2\Phi/\gamma_L^2 m$ and normalized harmonics of the Wigner function as

$$\frac{kg_n}{\gamma_L [\partial G_0(v_z)/\partial v_z]_{\omega/k}}$$

the coupled equations become

$$\frac{\partial \hat{\Phi}(t)}{\partial t} = \frac{1}{\pi} \int_{\text{res}} g_1 dv \quad (14)$$

$$\frac{\partial g_1}{\partial t} + ivg_1 = \hat{\Phi} \left[1 + \frac{g_0(v + \delta v_q) - g_0(v - \delta v_q)}{2\delta v_q} \right] + \hat{\Phi}^* \left[\frac{g_2(v + \delta v_q) - g_2(v - \delta v_q)}{2\delta v_q} \right] \quad (15)$$

$$\frac{\partial g_n}{\partial t} + invg_n = \hat{\Phi} \left[\frac{g_{n-1}^*(v + \delta v_q) - g_{n-1}^*(v - \delta v_q)}{2\delta v_q} \right] + \hat{\Phi}^* \left[\frac{g_{n+1}(v + \delta v_q) - g_{n+1}(v - \delta v_q)}{2\delta v_q} \right] \quad (16)$$

and

$$\frac{\partial g_0}{\partial t} = \hat{\Phi} \left[\frac{g_1^*(v + \delta v_q) - g_1^*(v - \delta v_q)}{2\delta v_q} \right] + \hat{\Phi}^* \left[\frac{g_1(v + \delta v_q) - g_1(v - \delta v_q)}{2\delta v_q} \right] \quad (17)$$

where $n \geq 2$ in Eq. (16) and the quantum velocity shift is $\delta v_q = \hbar k^2 / 2m\gamma_L$. We have omitted indices denoting normalized variables for notational convenience. Provided the conditions for the resonance region presented above is fulfilled, we may neglect perturbations at the boundary, i.e. use the approximation $g_n(\pm \delta v_{\text{res}}) \approx 0$ where $n = 0, 1, 2, \dots$. This property holds in the vicinity of the boundary (where the vicinity means a velocity of the order δv_q), which means that

$$\int_{\text{res}} g_0(v + \delta v_q) g_1^*(v) dv \approx \int_{\text{res}} g_0(v) g_1^*(v - \delta v_q) dv. \quad (18)$$

When δv_{res} is chosen large enough such that Eq. (18) is fulfilled, as well as similar types of approximations involving g_n , the system (14)-(17) posses an energy conservation law

$$\frac{\partial W_{\text{tot}}}{\partial t} = \frac{\partial}{\partial t} \left[|\hat{\Phi}(t)|^2 + \frac{1}{2} \int_{\text{res}} g_0^2 dv + \sum_{n=1}^{\infty} \int_{\text{res}} |g_n|^2 dv \right] = 0 \quad (19)$$

where W_{tot} is the total energy. The first term of Eq. (19) represents the wave energy (including the kinetic energy in the non-resonant region), whereas $\int_{\text{res}} |g_n|^2 dv$ represents the particle energy in the resonant region of each harmonic. Note that the zero:th harmonic get an extra factor 1/2, which is related to g_0 being real. In the numerical calculation made in the next section Eq. (19) has been used as test of the numerical scheme and a confirmation that δv_{res} has been chosen large enough. In particular it should be stressed that the quantities $\int_{\text{res}} |g_n|^2 dv$ is not sensitive to the exact choice of δv_{res} , since the integrand falls off rapidly away from the resonance. This can be tested by varying the parameter δv_{res} in the numerical code. We find that the relative values of the wave energy and resonant energy changes around 0.001 – 0.002 when the value of δv_{res} is changed a factor 1 – 3 within the bounds of the strong inequalities.

An advantage with the above system (14)-(17) is that solving the equations numerically we can follow the evolution taking time-steps that are larger than the inverse plasma frequency, as the equations contain only the slow time-scales, as opposed to the original Wigner-Moyal equation (3). Moreover, we only need to solve the equations in a small part of the velocity space, close to the resonance, which also makes Eqs. (14)-(17) easier to solve numerically. Finally, the spatial dependence is solved for analytically in (14)-(17), which also simplifies the numerics.

III. REMARKS ON THE LINEAR THEORY

Before we start with a numerical study, let us first make a few comments regarding the linear theory. As the equation stands, making a linearization of Eqs. (14)-(17) completely removes the quantity δv_q which encodes the quantum properties. Eq. (15) can then be integrated according to

$$g_1 = e^{-i\omega t} \int_0^t \hat{\Phi}(t') e^{i\omega t'} dt' + e^{-i\omega t} g_1(t=0). \quad (20)$$

For certain initial conditions $g_1(t=0)$ the integrals in Eqs. (14) and (20) can be solved analytically (see e.g. Ref. [27] for details), and for these cases we indeed have linear damping $\hat{\Phi} \propto e^{-t}$ which is written $e^{-\gamma_L t}$ in non-normalized units, where

$$\gamma_L = -\frac{\pi}{k} \frac{[\partial G_0(v_z)/\partial v_z]_{\omega/k}}{\int_{\text{nr}} \frac{\partial f_0/\partial v_z}{(\omega - k_z v_z)^2} d^3 v}. \quad (21)$$

The reason no effects due to the quantum treatment is seen here is the assumption of a modest quantum regime $k v_i^2 / \omega \gg \delta v_{\text{res}} \gg \hbar k / 2m$. These conditions apply for a resonance in the tail of the distribution, when the wavelength is not too short. Whenever these inequalities hold we can also use

$$G_0(v_z + \hbar k / 2m) - G_0(v_z - \hbar k / 2m) \simeq \frac{\hbar k}{m} \frac{\partial G_0}{\partial v_z} \quad (22)$$

which is the reason the finite difference is replaced by the classical expression containing a derivative in Eq. (21). Since g_0, g_1, g_2, \dots varies on a much shorter scale length in velocity space as compared to G_0 , we note that a similar approximation cannot be applied for these quantities. We stress that in a general scenario (e.g. for a beam-plasma system or for the regime $\hbar k^2/m \sim \omega$) the approximation (22) may give an incorrect description of linear Landau damping, but in our case the linear regime is classical to a good approximation. It should also be noted that the evolution of g_1 exhibits phase mixing due to the factors e^{-ivt} (see also Fig. 1 of the next section) whether or not the linear damping expression contains a finite difference or a derivative. Hence the quantum influence on the regime of linear Landau damping tend to be relatively modest also when the approximation (22) is avoided.

IV. NUMERICAL SOLUTIONS

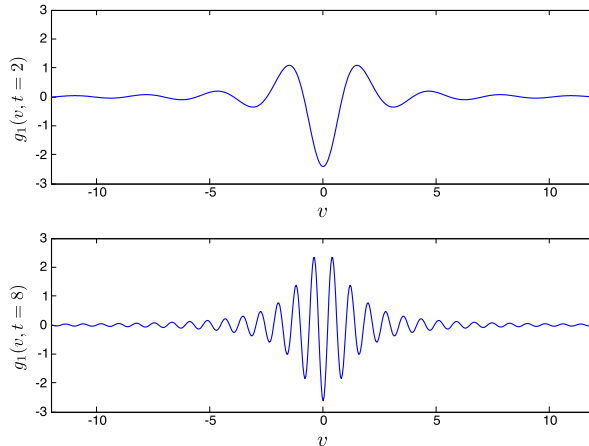


Figure 1. The real part of part of g_1 evaluated in the small amplitude regime for $t = 2$ (upper panel) and $t = 8$ (lower panel). The term ivg_1 of Eq. (15) leads to phase mixing, i.e. the development of increasingly small scales in velocity space. It should be noted that quantum effects does not counteract this behavior for small amplitudes.

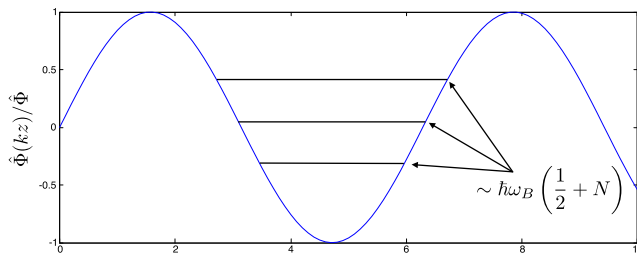


Figure 2. A qualitative illustration of the trapped particles. For a fixed wave amplitude particles trapped particles in the wave field have discrete energies, with an energy step of the order of $\hbar\omega_B$. When this becomes comparable to $q\hat{\Phi}$ only a few states are trapped, and quantum mechanical effects become important to describe the evolution.

The system (14)-(17) has been studied numerically using a staggered leapfrog finite differencing technique. Two

classes of initial conditions have been used. In the first case $g_1(v, t=0) = \hat{\Phi}(t=0)/(iv+1)$ and $g_0(t=0) = g_n(t=0) = 0$ (for $n \geq 2$). This has the advantage that the Wigner function approaches the value outside the resonance region for $v \gg 1$. The other choice is to put also $g_1(v, t=0) = 0$ such that the initial Wigner function is identically zero in the resonant region. It turns out that the evolution is almost completely independent of this difference in initial conditions, if the initial amplitude $\hat{\Phi}(t=0)$ is increased in the latter case such as to make the initial energy equal in the two cases. In what follows all numerical results will refer to the case with $g_1(v, t=0) = \hat{\Phi}(t=0)/(iv+1)$. Picking a small initial amplitude $\hat{\Phi}(t=0) \ll 1$ the system shows a damping $\hat{\Phi} \propto e^{-t}$ as expected due to the normalization of the time variable. As noted in the previous section the evolution is independent of the quantum parameter δv_q , which is related to the assumption $\hbar\omega/mv_t^2 \ll 1$ that was made in the derivation. Fig. 1 compares the real part of g_1 for different times. The evolution shows the evolution towards smaller scale lengths in velocity space due to phase mixing. When nonlinearities come into play this process plays part in increasing the relative importance of quantum effects in wave-particle interaction, as mathematically the system (14)-(17) differs from the classical limit once the scale length of g_n in velocity space is smaller than δv_q . However, a more physical way to understand why quantum effects become important more easily in the nonlinear regime than in the linear regime is shown in Fig. 2. Here as a rough approximation we have described the discrete eigenstates of trapped particles as that of an harmonic oscillator where the eigenfrequency is the bounce frequency ω_B . Naturally this is rather crude, as the electrostatic potential is only harmonic for the lowest energy states (if at all), and moreover the potential can vary dynamically to a smaller or larger degree depending on the parameters of the problem. Still the simple picture in Fig 2 is sufficient to identify one of the key parameters R_{tr} , which is the ratio of the trapping potential over the energy quanta of trapped particles, $R_{tr} = q\hat{\Phi}/\hbar\omega_B$. If the initial values have $R_{tr} \gg 1$ the evolution of the wave amplitude $\hat{\Phi}(t)$ is classical to a good approximation. On the other hand, when R_{tr} decreases towards unity the discrete energy states of the trapped particles will modify the evolution significantly. In terms of our normalized variables we note that the quantum trapping parameter can be written as $R_{tr} = q\hat{\Phi}/\hbar\omega_B = m\omega_B/\hbar k^2 = \hat{\Phi}^{1/2}/\delta v_q$. For $R_{tr} < 1$ we will not have trapped particles. However, as we will see below the close coupling between the existence of trapped particles and nonlinear evolution that holds in the classical regime does not generally apply in the quantum regime.

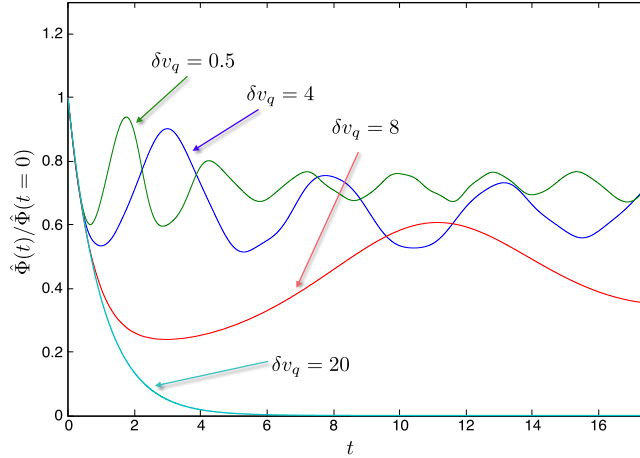


Figure 3. The evolution of $\hat{\Phi}(t)$ for initial amplitude $\hat{\Phi}(t=0) = 4$ and $\delta v_q = 0.5, 4, 8$ and 20 . The value $\delta v_q = 0.5$ gives a classical evolution to a good approximation, whereas for $\delta v_q = 20$ the nonlinearities are almost completely suppressed by the quantum effects.

Next we investigate how the value of the quantum parameter δv_q affects the evolution of $\hat{\Phi}(t)$ in the nonlinear regime. Keeping the normalized initial amplitude equal to $\hat{\Phi}(t=0) = 4$ (which means that the (initial) bounce frequency is $\omega_B = 2\gamma_L$), we follow the evolution up to $t = 17.5$ for various values of δv_q . The result is shown in Fig. 3. For $\delta v_q \lesssim 1$ the evolution of the wave amplitude more or less coincides with the classical case. This means that an initial drop in amplitude is followed by oscillations with a frequency of the order of the bounce frequency ω_B . As ω_B is not a constant, it is no surprise that these oscillations are slightly irregular. This result is in agreement with previous works on the classical case, see e.g. [25, 29, 30]. When the quantum parameter δv_q is increased, more of the wave energy is converted to the particles (the initial amplitude drop is larger) and the period of the amplitude oscillations become longer. Eventually when $\delta v_q = 20$ the initial amplitude drop is so large such that the evolution has become almost completely linear. Keeping $\delta v_q = 20$ and instead varying the initial amplitude, the evolution $\hat{\Phi}(t)$

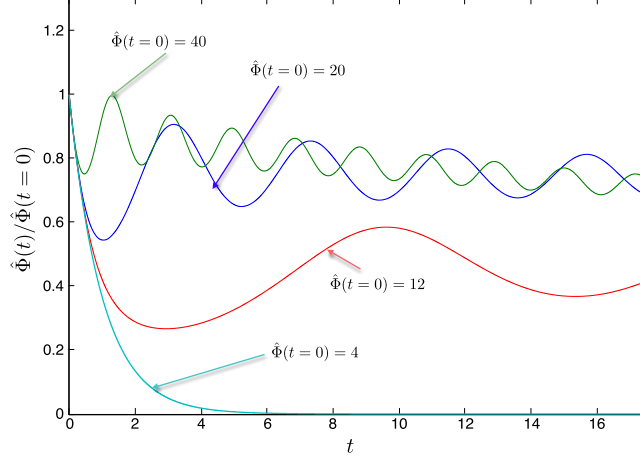


Figure 4. The evolution of $\hat{\Phi}(t)$ for $\delta v_q = 20$. The initial amplitudes are $\hat{\Phi}(t=0) = 4, 12, 20$ and 40 .

for various values of $\hat{\Phi}(t=0)$ is shown in Fig 4. The same qualitative features as in Fig 3 can be seen. That is the amplitude oscillation gets a lower frequency with decreasing $\hat{\Phi}(t=0)$, and the initial drop in wave amplitude is larger, until eventually for small enough initial amplitude the nonlinearities are suppressed and we obtain linear damping. A more quantitative analysis based on Figs 3 and 4 reveals that amplitude oscillations have a frequency $\omega_{\text{amp}} \sim (\omega_B^2/(1 + \delta v_q) - \gamma_L^2/2)^{1/2}$. Classically $\delta v_q = \hbar k^2/2m\gamma_L$ is small and $\omega_{\text{amp}} \sim \omega_B$ for $\omega_B/\gamma_L \gg 1$. When the quantum velocity shift δv_q becomes comparable to the characteristic scale of g_1 the frequency of the amplitude oscillations decreases. Still the amplitude may oscillate nonlinearly even for large δv_q and $R_{\text{tr}} \ll 1$ (in the regime of no trapped particles). The transition to linear evolution occurs when the expression for ω_{amp} becomes negative, in which case the amplitude oscillation frequency decreases too fast for the nonlinear oscillations to get started.

Next we look closer on some of the details of the numerical results. As shown in Figs 3 and 4, the evolution of the wave amplitude changes rather smoothly with δv_q . However, the various harmonics of the Wigner function g_n is more sensitive to the change in δv_q . The discrete structure involving momentum changes $\hbar k = 2m\delta v_q$ can be seen directly in the Wigner function, perhaps most clearly in g_0 . In a very rough sense there is a relation between the energy states displayed in Fig. 2 and the momentum structure shown in the upper panel of Fig. 5. As shown in Fig 5 where $g_0(v, t=10)$ is plotted in the classical and quantum mechanical regime, respectively, there is a very distinct difference between the quantum mechanical and classical regime. For the former case clear dips for $v \approx -\delta v_q$ and $v \approx -2\delta v_q$ can be seen, as well as peaks for $v \approx \delta v_q$ and $v \approx 2\delta v_q$. It should be noted, however, that a discrete structure in the momentum dependence can be seen even in the absence of trapped particles.

Another important aspect is the convergence in the sum over harmonics g_n , which is much faster in the quantum regime. A comparison of the classical and quantum regime is displayed in Fig. 6. We see that the relative amount of energy in the third harmonic $\int |g_3(t)|^2 dv/W_{\text{tot}}$ is changed dramatically when δv_q is changed from 0.5 to 4. The convergence in the sum over the harmonics is determined by the trapping parameter R_{tr} . In the classical and nonlinear regime with $R_{\text{tr}} \gg 1$ we need to include harmonics up to g_{10} , or even more. Besides the value of R_{tr} the number of harmonics needed depends on the degree of the nonlinearity and how long the evolution is followed. In the quantum regime when $R_{\text{tr}} > 1$ including up to g_3 is typically more than enough to get convergence. This applies even when $\omega_{\text{amp}} \gg \gamma_L$ and the evolution is strongly nonlinear. While the trapping parameter R_{tr} determines much of the properties of the Wigner function in the resonant region, it is the parameter $R_{\text{nl}} = \omega_B^2/[\gamma_L^2(1 + \delta v_q)] = \hat{\Phi}/(1 + \delta v_q)$ that determines the degree of nonlinearity. In the nonlinear regime $R_{\text{nl}} \gtrsim 1/2$ this parameter determines the frequency of the nonlinear amplitude oscillations, and we have $\omega_{\text{amp}}^2 = (R_{\text{nl}} - 1/2)\gamma_L^2$. For small R_{nl} (in practice $R_{\text{nl}} < 0.25$) the evolution is linear to a very good approximation. The reason why R_{nl} determines the nonlinearity can be understood roughly as follows: A key time-scale is the time-scale t_{char} for modifying the background distribution. Classically this time-scale is set by the inverse bounce-frequency, i.e. we have $t_{\text{char}}^2 \sim \omega_B^{-2} \propto \hat{\Phi}^{-1}$. Mathematically this simply reflects the fact that the coupling to g_0 and the higher harmonics g_n is linear in the wave amplitude, as seen in Eqs (15)-(17). When quantum effects enter the velocity derivative is replaced by a finite difference. Classically when the scale lengths in velocity space increases (cf Fig. 1) the magnitude of the nonlinear terms increases. However, the finite value of δv_q prevents the continuous increase of the nonlinear coupling, as is seen from Eqs (15)-(17), and effectively the transition from classical to quantum regime correspond to a change $\hat{\Phi} \rightarrow \hat{\Phi}/(1 + \delta v_q)$. Physically this

means that the characteristic time for acceleration of particles increases when the minimum velocity change comes in steps of $2\delta v_q$. Noting that $\gamma_L^2 t_{\text{char}}^2 > 1$ for the nonlinear modifications of g_0 to occur faster than the linear damping explains the significance of the parameter R_{nl} .

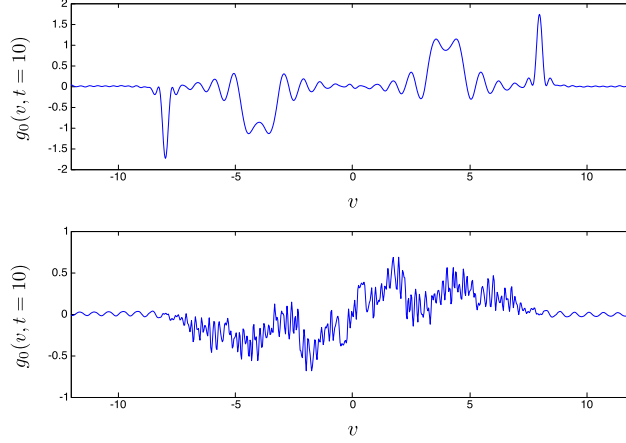


Figure 5. The profile of $g_0(v, t = 10)$ shown for initial amplitude $\hat{\Phi}(t = 0) = 4$ for $\delta v_q = 0.5$ (lower panel) and for $\delta v_q = 4$ (upper panel). The discrete nature of the velocity dependence with peaks at discrete values of δv_q is clear in the quantum regime. There is also a relation to the discrete energy states of Fig. 2, since the discrete velocity structure disappears when there is a large number of trapped states, as seen in the lower panel. However, there is not a one-to-one correspondence between the energy states and the velocity structure. Specifically the discrete structure of the velocity dependence can be present in the strong quantum regime when the particle trapping is absent due to quantum effects.

The results reported here are similar in some respects to the findings of Ref. [21] and Ref. [22]. In Ref. [21] the full Wigner equation was solved numerically. It was then found that the nonlinear regime of Landau damping was suppressed when $\hbar k / m v_t = 8$. This is a rather extreme quantum regime, and our condition for suppressing the nonlinear regime (essentially ω_{amp}^2 being negative) which roughly gives $\hbar k^2 / 2m > \omega_B^2 / \gamma_L$ is much easier to fulfill. The main reason for our relaxed quantum condition is that we have focused on a resonance in the tail of the distribution, where $\gamma_L \ll \omega$. In this case δv_q become comparable to the velocity scale length close to the resonance long before δv_q becomes comparable to the thermal (or Fermi) velocity. Thus we can investigate a regime where the wave-particle interaction is quantum mechanical, although the real part of the wave frequency is determined by the classical dispersion relation. By contrast, for a resonance in the bulk of the distribution, all quantum effects appear simultaneously. Next we compare our results with those of Ref. [22], that has studied the initial evolution of the wave particle interaction. We note that the comparison of the quantum time-scales $t_q = 2m / \hbar k^2$ with the classical bounce time $t_B = 2\pi / \omega_B$ made in [22] is very similar to the discussion made above. In particular Ref. [22] notes that the condition $t_q \ll t_B$ implies the absence of trapped particles. However, since Ref. [22] only studies the initial evolution, the conclusion that the nonlinear regime is suppressed for $t_q < t_B$ suggested in that work is not accurate. Using the notation of [22], rather the condition for suppressing the nonlinear regime is $t_q < t_B^2 \gamma_L$, as explained above.

Much of the above features can be summarized in Fig. 7 that shows the different regimes of Landau damping plotted as a function of the nonlinearity parameter ω_B / γ_L and the quantum parameter $\hbar k^2 / 2m \gamma_L$. The interesting part of the diagram is the nonlinear quantum regime $\omega_B / \gamma_L \geq 1$ and $\hbar k^2 / 2m \gamma_L \geq 1$. It should be noted that the condition for quantum suppression of the nonlinear amplitude oscillations given by Ref. [22] is the same condition that separates our region V from region VI (i.e. the condition that controls the existence of trapped particles). Interestingly, however, we find that the system can undergo nonlinear bounce-like oscillations even without trapped particles, and hence the region of quantum suppression (region IV) is determined by a distinct condition involving the quantum modified bounce frequency. It should be noted that the collisional influence can modify the different regimes to some extent. This will be discussed in some detail in the final section.

A feature of Fig. 4 not explained by the above discussion is the small but continuous decrease of wave energy seen for the highest amplitude in Fig. 4. Besides the amplitude oscillation there is a continuous decrease in $\hat{\Phi}(t)$ for initial condition $\hat{\Phi}(t = 0) = 40$ but not for $\hat{\Phi}(t = 0) = 20$. To understand this we must investigate how the energy of the particles in the resonance region is distributed among the harmonics. As described above the convergence is the sum over harmonics is fast for $R_{\text{tr}} = \sqrt{\hat{\Phi}} / \delta v_q \ll 1$. For the curves displayed in Fig 4 only the one with $\hat{\Phi}(t = 0) = 40$ has significant harmonic generation. For all the other curves the harmonics g_n for $n \geq 2$ is effectively not excited, and

the two terms $(1/2) \int_{\text{res}} g_0^2 dv + \int_{\text{res}} |g_1^2| dv$ accounts for more than 99% of the particle energy. However, due to the rapid phase mixing of g_2 for large δv_q , this harmonics does not return the particle energy to wave energy, but instead the second harmonic acts as a leakage of energy, not taking part in bounce-like oscillations. This can be contrasted against the oscillatory evolution of the energy of the third harmonic for $\delta v_q = 0.5$ which could be seen in Fig. 6. To a small extent the continuous loss of wave energy to higher harmonics can be observed also for $\hat{\Phi}(t=0) = 20$, but to a much smaller degree. This is illustrated in Fig 8, where the relative energy content in the second harmonic $\int_{\text{res}} |g_2^2| dv / W_{\text{tot}}$ is plotted for $\hat{\Phi}(t=0) = 20$ and for $\hat{\Phi}(t=0) = 40$. As can be seen, by a comparison with Fig. 4 the continuous increase of energy in the second harmonic accounts rather well for the overall downward trend in wave energy. A similar mechanism in principle exists also for lower values of δv_q . However here it is much less effective. The reason is twofold. Firstly, for lower δv_q the peaks of g_2 and higher harmonics occurs for a smaller velocity, and phase mixing is less effective. Thus the energy of the higher harmonics can be returned back to lower harmonics more easily. Secondly, for the same degree of nonlinearity (same value of R_{nl}) the trapping parameter is larger for smaller δv_q . Hence a larger number of harmonics are excited for lower δv_q . This means that the highest harmonic excited takes a smaller proportion of the energy, in which case the leakage of energy is smaller. In practice, the details of the energy loss is likely to be determined by collisional effects, as very small scales in velocity space develops during the evolution [25].

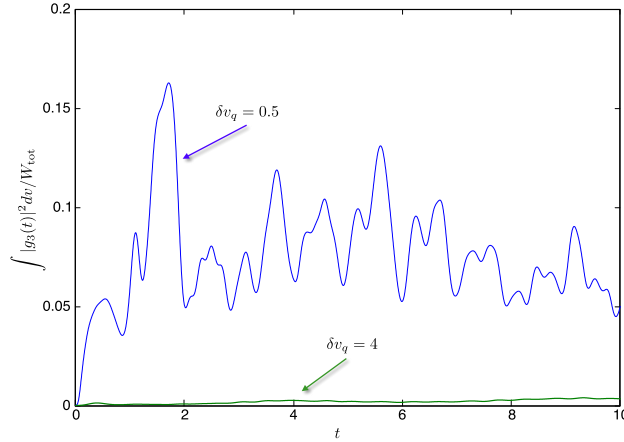


Figure 6. Comparison of the relative energy in the third harmonic $\int |g_3(t)|^2 dv / W_{\text{tot}}$ for initial amplitude $\hat{\Phi}(t=0) = 4$. The two curves are computed for $\delta v_q = 0.5$ and for $\delta v_q = 4$ respectively.

V. SUMMARY AND DISCUSSION

Usually particle dispersive effects as accounted for by the Wigner-Moyal equation are assumed to be significant when the thermal de Broglie length $\lambda_{\text{dB}} = \hbar / mv_t$, or its counterpart for a degenerate plasma, \hbar / mv_F (where v_F is the Fermi velocity), becomes comparable to the Debye length $\lambda_D = v_t / \omega_p$ (or v_F / ω_p). The physics behind this condition is that the importance of collective effects require scale lengths not much shorter than the Debye length, and for the sinus-operator in Eq. (3) not to reduce to its classical limit we need $\hbar L_{\text{char}}^{-1} / mv_{\text{char}} \sim 1$. If the characteristic spatial scale length L_{char} is assumed not to be smaller than λ_D , and the velocity scale length v_{char} is of the order of v_t we get the condition $\hbar \omega_p / mv_t^2 \sim 1$ (or $\hbar \omega_p / mv_F^2 \sim 1$ for a degenerate plasma) for quantum effects to be significant [1–3]. This condition applies broadly to many situations, but does not hold for wave-particle interaction in general, as we have $v_{\text{char}} \ll v_t$ in case the resonance lies in the tail of the distribution. In the present paper, focusing on the case of Langmuir waves of a single wavelength, we have found that quantum effects become important in the nonlinear regime once $\hbar k^2 / m \sim \omega_B$ in which case the trapped particle energies are quantized. Already when $\hbar k^2 / m > \gamma_L$ nonlinear oscillations at the bounce frequency is slowed down in accordance with $\omega_B \rightarrow \omega_B / (1 + \delta v_q)^{1/2}$. While these oscillations are qualitatively similar to the well-known bounce oscillations [29], it should be noted that in the quantum regime such oscillations can occur even in the absence of trapped particles. Increasing the quantum parameter δv_q even further, eventually the nonlinear oscillations are suppressed when $\omega_B / (1 + \delta v_q)^{1/2} < \gamma_L$ in which case usual linear damping takes place.

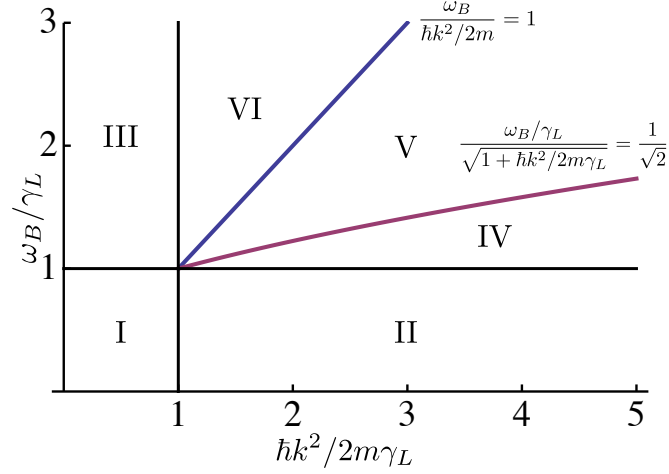


Figure 7. Summary of the different regimes of Landau damping for a resonance in the tail. Region I and II: Linear Landau damping. The quantum effects in region II does not change the value of the linear damping for a resonance in the tail Region III: Classical nonlinear regime with bounce oscillation of frequency $\sim \omega_B$. Region IV: Quantum suppression of nonlinear bounce-like oscillations. Region V: Nonlinear regime with bounce-like oscillations in the absence of trapped particles Region VI: Region of trapped particles with quantum modified bounce oscillations. Note that the same expression $\sim \omega_B / (1 + \hbar k^2 / m \gamma_L)^{1/2}$ for the quantum modified amplitude oscillations apply in both region V and VI

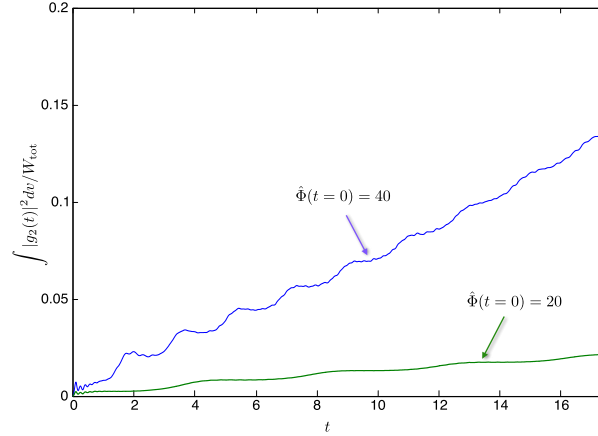


Figure 8. Comparison of the relative energy in the second harmonic $\int |g_2(t)|^2 dv / W_{\text{tot}}$ for $\delta v_q = 20$. The two curves are computed for initial amplitude $\hat{\Phi}(t=0) = 20$ and $\hat{\Phi}(t=0) = 40$ respectively.

Since the phenomena of study evolves on a time scale slower than the plasma frequency, the above picture can be modified when the collisional influence is accounted for. Let us illustrate this by considering a concrete example. First we note that the long term evolution will always be affected by collisions. The characteristic time scale for collisions to be important τ_c is given by $\min[\nu_{ei}^{-1}, \nu_{ee}^{-1}]$. To some extent we can assure that the phenomena of study occur on a faster scale by picking a relatively large amplitude and avoiding a resonance too far out in the tail of the distribution. However, for a strongly coupled plasma this will not suffice, as ν_{ee} approaches the plasma frequency rather than being a small parameter. Thus for our model to apply we must first of all consider a plasma that is weakly coupled. As an example we pick a plasma with a number density $n_0 \simeq 10^{28} \text{m}^{-3}$ and a temperature $T \simeq 10^7 \text{K}$ that correspond to a coupling parameter $\Gamma \simeq 0.01$. Such parameter values may result from laser-plasma experiments, see e.g. Ref. [17]. Furthermore the temperature is well above the Fermi temperature, and we have a Debye length of the order $\lambda_D \simeq 10^{-9} \text{m}$. Adjusting the wavenumber we can choose the amount of resonant particles that determine the linear Landau damping rate and thereby pick the quantum parameter. In order to get $\delta v_q \simeq 4$ we can aim at $\gamma_L \simeq 10^{12} \text{s}^{-1}$

which is obtained for a wave number $k \simeq 2 \times 10^8 \text{m}^{-1}$. As $\delta v_q > 1$ we are well in the quantum regime. We note, however, that although the plasma is weakly coupled, the time-scale for collisional damping is still shorter than the linear damping time γ_L^{-1} . This is typically the case in the quantum regime, and hence the long-time evolution is generally much affected by collisions. However, most of our findings concern the *nonlinear* quantum behavior. As we will demonstrate below these findings are to a large extent still relevant even when collisions are taken into account. Firstly, the quantum modified bounce frequency $\omega_B \rightarrow \omega_B/(1 + \delta v_q)^{1/2}$ can be experimentally verified after a few bounce oscillations. For example, if we pick $\hat{\Phi} \gtrsim 10V$ the bounce oscillations take place on a much faster scale than collisional damping, in which case the quantum modification of the bounce frequency becomes detectable. Moreover, generally the prediction of a nonlinear regime in the absence of trapped particles (regime V in Fig. 7) can be verified after a few (quantum modified) bounce oscillations. Hence in an experimental situation we do not need to follow the evolution until collisional effects become important. The situation is somewhat different when it comes to the condition for quantum suppression of the nonlinear oscillations. It is possible to verify that previously given conditions are incorrect in agreement with our theory, as the presence of bounce oscillations at a faster scale than the linear damping rate will confirm this. However, the quantitative confirmation of our condition that separates regions IV and V in Fig 7 is likely not possible, as that would require us to study the system when the quantum modified bounce frequency is of the same order as the linear Landau damping rate. In this case we need to follow the evolution long enough such that collisions will modify the picture. Thus we conclude that most features of Fig 7 remains even when we account for collisional effects, but that there are restrictions arising from the collisional influence that makes the boundary between region IV and V uncertain.

While the study here has focused on Landau damping due to electrons, it should be noted that a similar process may take place for photons [26, 31]. Photon Landau damping can be relevant to Langmuir waves with relativistic phase velocities, in the presence of electromagnetic radiation, when resonant electrons are nearly absent. The wave nature of the photons provides the classical counterpart to the quantum electron states, and we can similarly identify a photon bounce frequency $\omega_{Bph} \sim \omega_B$. Photon trapping effects were experimentally observed by [32].

Acknowledgement This paper is dedicated to our good friend and colleague Professor Lennart Stenflo, celebrating his 75:th birthday.

-
- [1] G. Manfredi, Fields Inst. Commun. **46**, 263 (2005).
 - [2] F. Haas, *Quantum Plasmas, A Hydrodynamics Approach* (Springer, New York, 2011).
 - [3] P. K. Shukla and B. Eliasson, Rev. Mod. Phys. **83**, 885 (2011).
 - [4] A. Bret, Phys. Plasmas **14**, 084503 (2007).
 - [5] P. A. Andreev, L. S. Kuzmenkov and M. I. Trukhanova, Phys. Rev. B, **84**, 245401 (2011)
 - [6] F. Sayed, S. V. Vladimirov, Yu. Tyshetskiy and O. Ishihara, Phys. Plasmas **20**, 072116 (2013)
 - [7] G. Brodin and M. Stefan, Phys. Rev. E **88**, 023107 (2013).
 - [8] M. Marklund, G. Brodin, L. Stenflo and C. S. Liu, Europhys. Lett, **84**, 17006 (2008).
 - [9] P. K. Shukla and L. Stenflo, J. Plasma Phys., **74**, 575 (2008).
 - [10] N. Crouseilles, P. -A Hervieux and G. Manfredi, Phys. Rev. B, **78**, 155412 (2008).
 - [11] J. Zamanian, M. Marklund and G. Brodin, Phys. Rev. E **88**, 063105 (2013).
 - [12] J. Zamanian, M. Marklund, G. Brodin, New J. Phys. **12**, 043019 (2010).
 - [13] J. Lundin and G. Brodin, Phys. Rev. E **82**, 056407 (2010).
 - [14] F. A. Asenjo, V. Munoz, J. A. Valdivia and S. M. Mahajan, Phys. Plasmas **18**, 012107 (2011).
 - [15] J.T. Mendonça, Phys. Plasmas **18**, 062101 (2011).
 - [16] G. Manfredi and P.-A. Hervieux, Appl. Phys. Lett. **91**, 061108 (2007).
 - [17] S. H. Glenzer and R. Redmer, Rev. Mod. Phys. **81**, 1625 (2009).
 - [18] A. K. Harding and D. Lai, Rep. Prog. Phys. **69**, 2631 (2006).
 - [19] H. A. Atwater, Sci. Am. **296**, 56 (2007).
 - [20] S. A. Wolf, D. Awschalom, R. A. Buhrman, *et al.*, Science **294**, 1488 (2001).
 - [21] N. D. Suh, M. R. Feix and P. Bertrand, J. Compl. Phys. **94**, 403 (1991).
 - [22] J. Daligault, Phys. Plasmas, **21**, 040701 (2014).
 - [23] A. Luque, H. Schamel and R. Fedele, Phys. Lett. A, **324**, 185 (2004).
 - [24] F. Haas, B. Eliasson, P. K. Shukla, and G. Manfredi, Phys. Rev. E., **78**, 056407 (2008).
 - [25] G. Brodin, Phys. Rev. Lett. **78**, 1263 (1997).
 - [26] J. T. Mendonça, *Theory of Photon Acceleration*, (Bristol: Institute of Physics publishing, 2001).
 - [27] G. Brodin, Am. J. Phys. **65**, 66 (1997).
 - [28] The staggered leapfrog method also works well when the finite differences in the right hand side is replaced by a velocity derivative, which corresponds to the classical limit. In the quantum regime Eqs. (15)-(17) just constitute a set of ordinary differential equations (although it is a large set, since the velocity resolution must be sufficient), and a fourth order Runge-Kutta method could also be applied.

- [29] T. M. O’Neil, Phys. Fluids **8**, 2255 (1965).
- [30] G. Manfredi, Phys. Rev. Lett. **79**, 2815 (1997).
- [31] J. T. Mendonça and A. Serbeto, Phys. Plasmas **13**, 102109 (2006).
- [32] C. Murphy *et al.*, Phys. Plasmas **13**, 033108 (2006).